AN INVESTIGATION

OF THE CHARACTERISTICS

OF A PULSED MERCURY ARC

by

HUGH DANIEL CAMPBELL

B.Sc., University of British Columbia, 1962

A THESIS SUBMITTED IN PARTIAL FULFILMENT OF

THE REQUIREMENTS FOR THE DEGREE OF

MASTER OF SCIENCE

in the Department

of

PHYSICS

We accept this thesis as conforming to the

required standard

THE UNIVERSITY OF BRITISH COLUMBIA

March, 1965

In presenting this thesis in partial fulfilment of

the requirements for an advanced degree at the University of

British Columbia, I agree that the Library shall make it freely

available for reference and study. I further agree that per-

mission for extensive copying of this thesis for scholarly

purposes may be granted by the Head of my Department or by

his representatives. It is understood that copying or publi-

cation of this thesis for financial gain shall not be allowed

without my written permission.

Department of PHYSICS

The University of British Columbia,
Vancouver 8, Canada

Date March 10, 1965.

ABSTRACT

An investigation of a pulsed Hg arc has been undertaken to test the relation $V \alpha I^{.4}$ between the voltage and current of an arc discharge. Although the experimental V-I characteristic exhibited this tendency, further considerations strongly indicated that the agreement between theory and experiment was probably a coincidence.

The Paschen breakdown curve was determined, and together with simultaneous measurements of the current and voltage, it was possible to measure the average column field strength as a function of current.

As a result of an unexpected feature of the apparatus, namely an inherent motion of the electrodes, the voltage waveform could be used to obtain an approximate measurement of the combined thickness of the anode and cathode falls d_f, and also the average field strength in these regions E_f. The measurements $d_f = 3 \times 10^{-6}$ cm, and $E_f = 2.4 \times 10^6$ volt/cm appear to be in agreement with the field emission theory.

ACKNOWLEDGEMENT

TABLE OF CONTENTS

LIST OF ILLUSTRATIONS

INTRODUCTION

The work described in this thesis started in an attempt
to verify the relation

$$V \propto I^{.4}$$

between the voltage V and current I in an arc discharge. This
relation had previously been shown
to be valid by Smy (1963) for cur-
rents passing through a shock heated
plasma. In order to derive this
expression, and also to interpret
the data, it had been found neces-
sary to assume a small conducting
spot on the cathode. As cathode spots are a well known pecu-
liarity of arcs it was felt that this shock tube expression might
also apply to the V-I characteristic of an arc. If so, this
equation would be a useful tool in arc physics, as no analyti-
cal expression for the over all characteristic is yet known,
although arcs have been studied extensively during the past cen-
tury. In order to test this relation, a pulsed arc experiment
was designed which would retain the short time feature of the
shock tube. The current pulse was supplied by the discharge of
a condensor through a current limiting resistor is series with
the arc.

It was found that a general knowledge of arcs was required
to interpret different features of the experimental results.
And, as an examination of Smy's theory would necessarily require

Figure 1   Shock Tube
           Arrangement

comparison with theoretical aspects of arcs, the following Chap-
ter 1 was included in this thesis to present a brief summary
of accepted experimental results and theoretical concepts of
arc physics.

Chapter 2 discusses details of the apparatus, as well as
the different measuring techniques employed. In particular,
an unexpected motion of the electrodes is examined in detail,
and a mechanism is suggested which describes the origin of this
motion.

Chapter 3 goes on to discuss the more general results which
were obtained in this project. These include the over all V-I
characteristic, the E_{co}-I characteristic (where E_{co} is the col-
umn field strength), and an order of magnitude measurement of
the average field strength in the fall regions. Although this
last measurement is not very precise, it would appear to be the
most significant result of this thesis (1965).

Chapter 4 contains a detailed examination of the theory
developed by Smy (1963). The object of this section is to see
to what extent the results obtained by Smy could apply to an
arc.

CHAPTER 1 - GENERAL FEATURES OF THE ELECTRIC ARC

Electric arcs have been studied extensively during the past century and so it might appear surprising that there are many features of an arc which are yet to be satisfactorily explained. While many of the individual processes such as production of charge carriers, or energy dissipation by radiation and heat conduction, can be understood in an isolated manner, it is difficult to combine these separate processes into a unified theory. Difficulties arise when analyzing experimental data, as the extraction of relevant parameters is often questionable. As a result of these problems of complexity, several different models and theories concerning arcs have been proposed. This chapter will present some of the experimentally observed characteristics of arcs, and will also discuss some of the presently well accepted theories.

1.1 EXPERIMENTAL OBSERVATIONS

The most important feature of the electric arc is the over all current-voltage characteristic. A typical case is shown schematically in Figure 2 (Goldman, 1961). The resultant non-linear characteristic is quite different from that of a standard ohmic resistor. For lower currents, the arc voltage falls very rapidly to some minimum voltage V_m, and then slowly rises again for increasing higher values of current. If the applied voltage falls below V_m the arc will extinguish - as a well known example, one can extinguish an arc by drawing the electrodes apart. It can also be seen that arcs of different lengths have the same general behavior, the longer arcs requiring a higher

applied voltage for a particular current.

The potential variation between the anode and cathode of a typical arc is given schematically in Figure 3 for two different values of current (Ecker, 1961). This figure indicates that there are three main regions of an arc; the cathode region (with net voltage drop V_c), the long central column region (V_{co}), and the anode region (V_a).

The problems associated with the electrode regions are frequently classified according to the boiling point of the electrode material. Thermal arcs, such as those formed with tungsten or carbon electrodes (high boiling point metals), have very different properties from those of cold cathode arcs such as mercury or copper (low boiling point metal electrodes). As this thesis deals solely with a cold cathode arc all details presented henceforth will apply only to this class of arcs.

The cathode fall voltage (V_c) of an arc is generally of the same order of magnitude as the ionization potential of the cathode vapour (typically around 10 volts; Brown, 1961). Experiments have shown that V_c is relatively independent of the current flow (Gerthsen and Schulz, 1955), and it is generally accepted that V_c acts over a distance comparable with the mean free path of the surrounding gas, although no successful measurement of this has been made. Two techniques have been used to determine values for the fall voltages, V_c, V_a, and $V_f = V_c + V_a$. First, extrapolating the linear region of Figure 3 in both directions gives approximate values for V_c and V_a. However this approach requires that the potential variation across the column
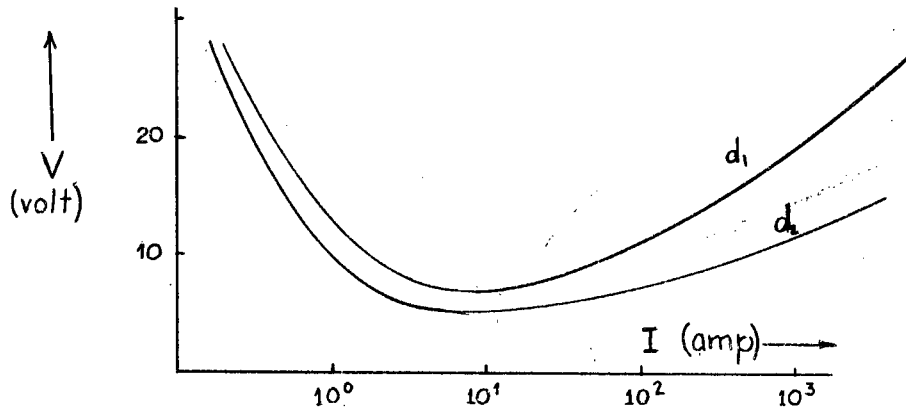
Figure 2 Voltage-Current Characteristic (schematic) of an Arc for two electrode separations with $d_1 > d_2$.
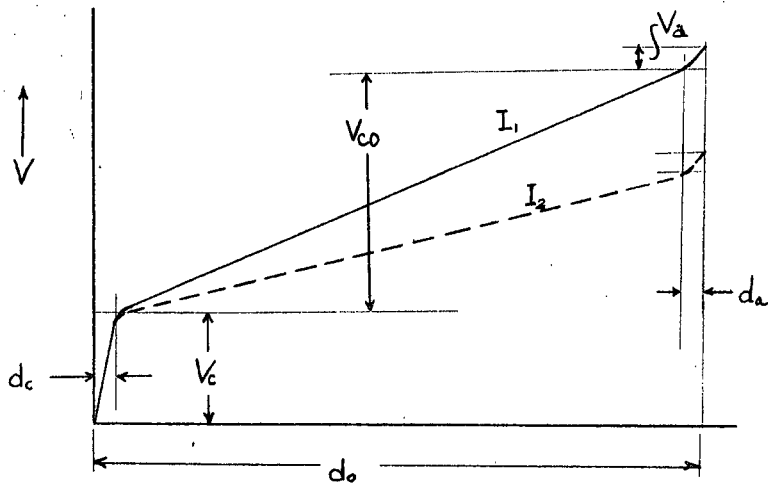

Figure 3 Potential Variation between Electrodes (schematic)

V_c, cathode fall voltage; V_a, anode fall voltage; V_{co}, column voltage drop; d_c, cathode fall distance; d_a, anode fall distance; d_o, total electrode separation.

be determined (see figure 3 again), and this is a difficult experimental task involving probe measurements (Hinrichs and Wienecke, 1959). A second and more direct approach is to bring

the two electrodes slowly together so that V_f can be measured just before touching (Gerthsen and Schulz, 1955). By taking several trials with different electrode materials, it is possible to extract values for V_a and V_c from the measurements of V_f. A variation of this
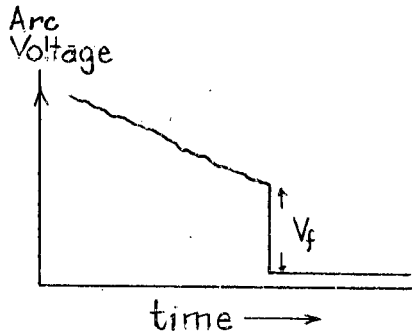
Figure 4   Determination
of V_f

second technique was used in this experiment to obtain an order of magnitude value for the sum of the fall distances, $d_f = d_c + d_a$ (see Section 3.1). It has been found by both methods that the anode fall voltage is much smaller than the cathode fall voltage ($V_a \cong V_c/10$; Bauer and Schulz, 1954), and will generally be neglected for our purposes.

The current at the cathode is concentrated into a small, highly luminous area A_s known as the cathode spot. Many attempts have been made to measure A_s, and it appears that as measuring techniques have improved the value obtained has gone down accordingly. If the current and spot area are measured simultaneously, then the current density j in the cathode spot can be calculated. Probably the most reliable measurements were obtained by Froome (1950). Using kerr cell photography on short duration arcs he found that $j = 10^6 \text{ amp/cm}^2$.

The most visible part of the arc is the arc column, which

serves as a current conducting path between the anode and cathode. The important properties of this region have been very success-fully examined by spectroscopic analysis and probe techniques. The main features of interest can be related to the radial tem-perature profile. These include the electrical and thermal conductivities, which strongly affect the column field strength E_{co} by their control on the rate of energy dissipation. As shown in Figure 3, E_{co} is constant over the length of the column, and hence can be determined by

$$E_{co} = \frac{V_{co}}{d_{co}} = \frac{V_{co}}{d_o} ,$$

as $d_f \ll d_o$ by many orders of magnitude. Although independent of column length, E_{co} is highly dependent upon the magnitude of the current. Most experiments which have measured this depen-dence have involved the use of probes in the lower current ranges. The experiment described in this thesis describes an approximate technique to determine $E_{co}(I)$ in the high current range.

1.2 THEORETICAL CONSIDERATIONS

The theoretical aspects of arcs can be classified in the same manner as was used when considering the experimental ob-servations. Models and theories describe either the column or the fall regions (in particular the cathode fall region). And again, the most formidable problems have been encountered in explaining the behavior of the electrode region rather than in the column region.

The basic problem to be solved in the electrode region is to determine the mechanism responsible for extraction of elec-

trons out of the cathode. The original proposition of thermionic emission by Richardson has been shown to be applicable to metals of very high boiling points. However, for low boiling point metals it is impossible to reach temperatures sufficiently high for appreciable thermal emission to occur. Several theories have been put forth, such as photo-electric emission, or emission due to metastable atoms (von Engel, 1957), or various combinations of two different mechanisms (see Ecker for a summary of the different proposals, 1951). However the field emission model by Longmuir and Mackeown (1929) appears to have been the most satisfactory to a fairly large number of workers. The important features of this model will now be briefly discussed.

The high positive space charge accumulation, which produces the cathode fall voltage, results in a very intense electric field at the surface of the cathode. Employing Poisson's equation and assuming the length of the cathode fall to be one mean free path, Mackeown derived the following expression,

$$E_c^2 = 7.57 \times 10^5 \, V_c^{1/2} \, j \left\{ (1-\gamma)(1845)^{1/2} - \gamma \right\} \qquad \ldots (1)$$

where, E_c = electric field at cathode surface (volt/cm)

V_c = cathode fall voltage

j = total current density in the fall region (amp/cm^2)

γ = ratio of $\dfrac{\text{electron current density}}{\text{total current density}}$.

The experimental verification of this equation has been very difficult as both j and γ have to be measured.

Wasserab (1951) used the Fowler Nordheim equation (1928) together with Mackeown's equation to show that γ was uniquely

determined as a function of j. For a Hg cathode he found that a current density of the order of 10^7 amp/cm^2 was required to produce appreciable field emission of electrons. While the theoretical result requires a current density of 10^7 amp/cm^2, the available experimental data can only show a lower limit of 10^6 amp/cm^2 and hence it is not possible to completely accept or reject the field emission model for the case of low boiling point metals.

The structure of the arc column has been examined by many workers, and the different approaches appear to be in reasonable agreement with each other, as well as with experimental observations. The first investigations were carried out by Schottky (1925). Considering the electrons, ions, and neutrals as interdiffusing gases, he obtained a mobility equation which described the general macroscopic behavior fairly well. Maecker developed a much more extensive theory by considering the energy balance in the column,

electrical energy input = energy lost by conduction

and radiation.

Neglecting the radiation term this equation can be solved for $E_{co}(I)$ if the electrical and thermal conductivities are known as functions of temperature. For the case of a cylindrically symmetric discharge with a monatomic gas, Maecker found that

$$E_{co} \propto I^{.4}, \qquad \qquad \dots(2)$$

and this equation was found to agree with the experimental measurements (Maecker, 1959). Unfortunately, the condition that radiation losses are negligible limits the application of this

equation (see Section 3.2).

As shown above, some features of the arc are fairly well understood, but it is interesting to note that very little successful work has been reported on the determination of an analytical expression describing the V-I characteristic of the arc. As recently as 1961 empirical curve fitting was still being used (Goldman, 1961). In view of this fact, all models which can be used to explain any portion of the caracteristic are of interest to the general theory of arcs.

In his work on shock-tubes Smy developed an expression for the V-I characteristic of two electrodes immersed in a shock-heated plasma. Experimental results indicated that in the high current range, production of electrons in the electrode region was probably accomplished by a conducting spot identical to the cathode spot of an arc. Using Mackeown's field emission equation he found

$$V \propto I^{.4}, \qquad \qquad ...(3)$$

which is similar to the result obtained by Maecker.

It was felt that the similarities, both in assumptions used and results obtained, between this model and accepted ideas on arcs were suffieient to warrant experimental examination in the high current range. The apparatus and experimental techniques used in this experiment will now be discussed in the following chapter.

CHAPTER 2 - APPARATUS AND EXPERIMENTAL DETAILS

2.1 DESIGN FEATURES OF APPARATUS

The apparatus designed for holding the Hg electrodes is shown in Figure 5. It consists of a vessel for the cathode pool (2.5 cm diameter), and a long tube for suspending the anode hemisphere (.3 cm inner diameter). Two pieces of tungsten wire (.1 cm diameter and 5 cm long) were inserted through the glass to allow contact of the Hg electrodes with the external circuit. The cathode pool was connected to a second pool P by a piece of tygon tubing. A lucite rod was fitted into the second pool and could be inserted to any desired depth. This motion could then be used to provide a fairly sensitive method for raising or lowering the level of the cathode pool.

One advantage of using Hg electrodes over solid metal electrodes is that one can establish clean surfaces with reproducible geometry very easily. After each discharge a new surface on the upper electrode was formed by allowing a small portion of Hg to flow down the tube. This ensured a clean anode before each discharge took place. The lower electrode could also easily be cleaned by lowering vessel P to such a level that the lower electrode was completely enclosed in the tygon tubing. All of the surface contamination then adhered to the tubing when P was raised again to its normal position.

A serious disadvantage encountered while using the liquid was the fact that during the course of a discharge the gap separation was continually changing. Complications dealing with this difficulty will be discussed in Sections 2.4 and 2.5.
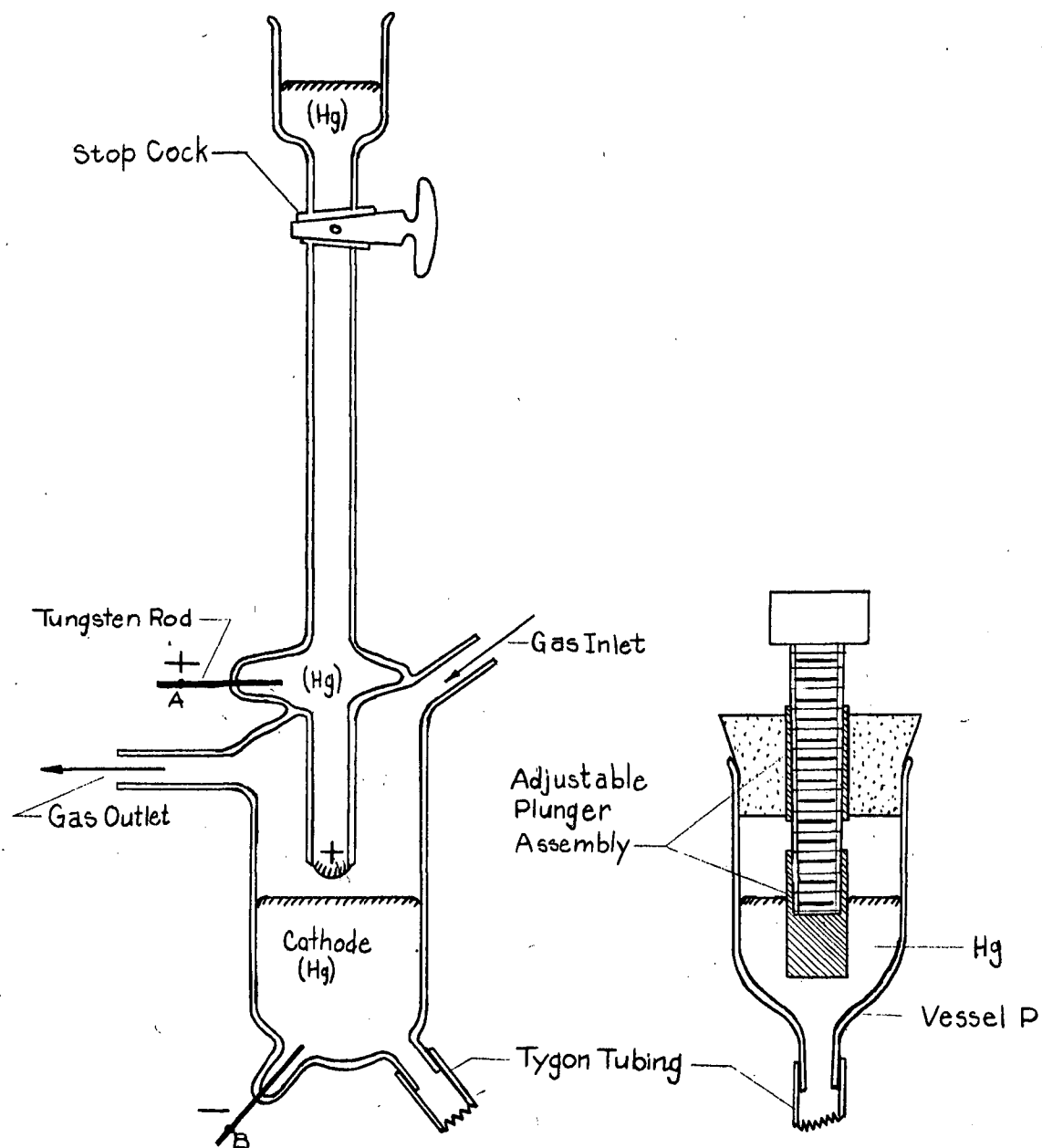
Figure 11 Apparatus Containing Mercury Electrodes

2.2 ELECTRICAL MEASUREMENTS

A general arrangement of the electrical circuit is given in Figure 6. The values quoted for the various circuit components are those which were most frequently used throughout the course of the experiment. A regulated power supply, continuously variable from 100-1500 volts, was used in series with a large charging resistor R_1 and a mechanical switch. A schematic diagram of the discharge circuit is given in Figure 7. The current waveform in the time interval 2-70 μsec was that of a simple RC decay for all practical purposes. This was verified by the measuring technique described in Appendix A, and was found to hold to within 3%.

The inherent inductance L_i of the circuit could be determined by observing the current waveform and measuring the time of maximum current T_m. Assuming L_i to be small enough to satisfy the condition

$$R^2 \ll \frac{4L_i}{C}$$

then T_m is related to L_i by

$$T_m = \frac{L_i}{R} \ln \frac{R^2 C}{L_i}$$

as shown in Appendix A. Using the values of R and C given in Figure 6, and a typical value of 2 μsec for T_m, L_i was found to be approximately .75 μh.

The current was determined by measuring the voltage drop across the series resistor R. Simultaneously, the voltage V_{AB} between points A and B (see Figure 8) was measured. In order

Figure 6   Arrangement of Electrical Circuit
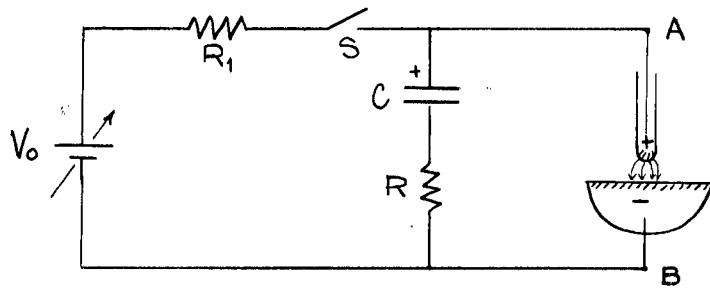
V_O, variable power supply; R_1(200 kΩ),
charging resistor;   S, mechanical switch;
C(30 μf), condensor bank;   R(.96Ω), current
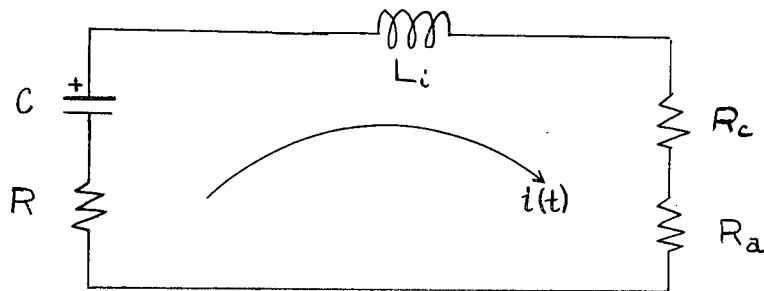measuring resistor;   A, lead to anode;
B, lead to cathode.

Figure 7   Schematic of Discharge Circuit

R_a, arc resistance; R_c, contact resistance;
L_i(.75 μh), inherent inductance of circuit;
R, as shown in Figure 6.

to determine the arc voltage it was necessary to know the voltage drop across the tungsten rods and the Hg, as the resistance of this part of the circuit is comparable with the resistance of the arc itself.

The circuit used to measure R_c is shown schematically in Figure 8. This value of resistance is in fact a sum of three resistances; the resistance of the tungsten rods, the resistance of the contact
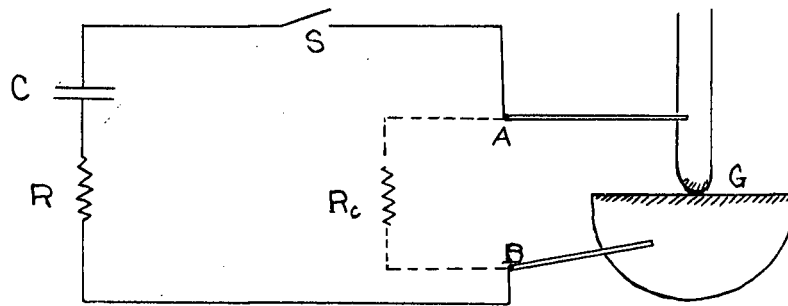
Figure 8   Schematic Circuit of R_c

R(.96 Ω), Series Resistor; C(30 μf), Capacitor; S, Mechanical Switch; A, Tungsten rod to anode; B, Tungsten rod to cathode; G, Hg bubble in contact with Hg pool; R_c, Contact resistance.

between the tungsten and Hg, and the resistance of the cold stationary Hg between the contacts. The bubble was lowered until complete contact with the pool was made. The current and corresponding voltage were displayed on a 536 Tektronix oscilloscope. By measuring the slope of the resulting oscillograms for several shots, R_c was found to be .012 Ω. In comparison, a typical resistance of the arc was .05 Ω.

In addition to the oscilloscope mentioned above, a dual-beam 551 Tektronix oscilloscope was used to measure the voltage-

time and the current-time relationship.

2.3 PASCHEN CURVE

An important parameter of arc discharges is the electrode separation d_o. In this experiment d_o was not an independent variable, but instead, was determined by initial conditions. The arc was initiated by a sparking mechanism, which resulted when a high electrostatic potential V_o was applied between the electrodes. The relationship between V_o and d_o should be given by standard Paschen curves. However, as there are many factors involved, it was necessary to measure this curve for the particular conditions of this experiment.

The electrical curcuit used in this measurement was identical to that shown in Figure 6. As the breakdown voltage V_o is independent of the discharge current it was more convenient to use a smaller capacitor (.002 μf), and a larger resistor (10 Ω). This combination ensured that the surfaces would remain relatively clean throughout this set of measurements, although this was not essential. A calibrated eyepiece was used with a cathetometer to measure the gap separation which was accurate to $\pm$ .005 mm. Within the range of measurements used this ensured a maximum instrument error of $\pm$ 5%.

The most common method of measuring the Paschen curve is to fix the distance and observe the corresponding breakdown voltage. As breakdown phenomena is statistical in nature, several shots must be taken at a particular distance to determine the correct sparking voltage. This approach turned out
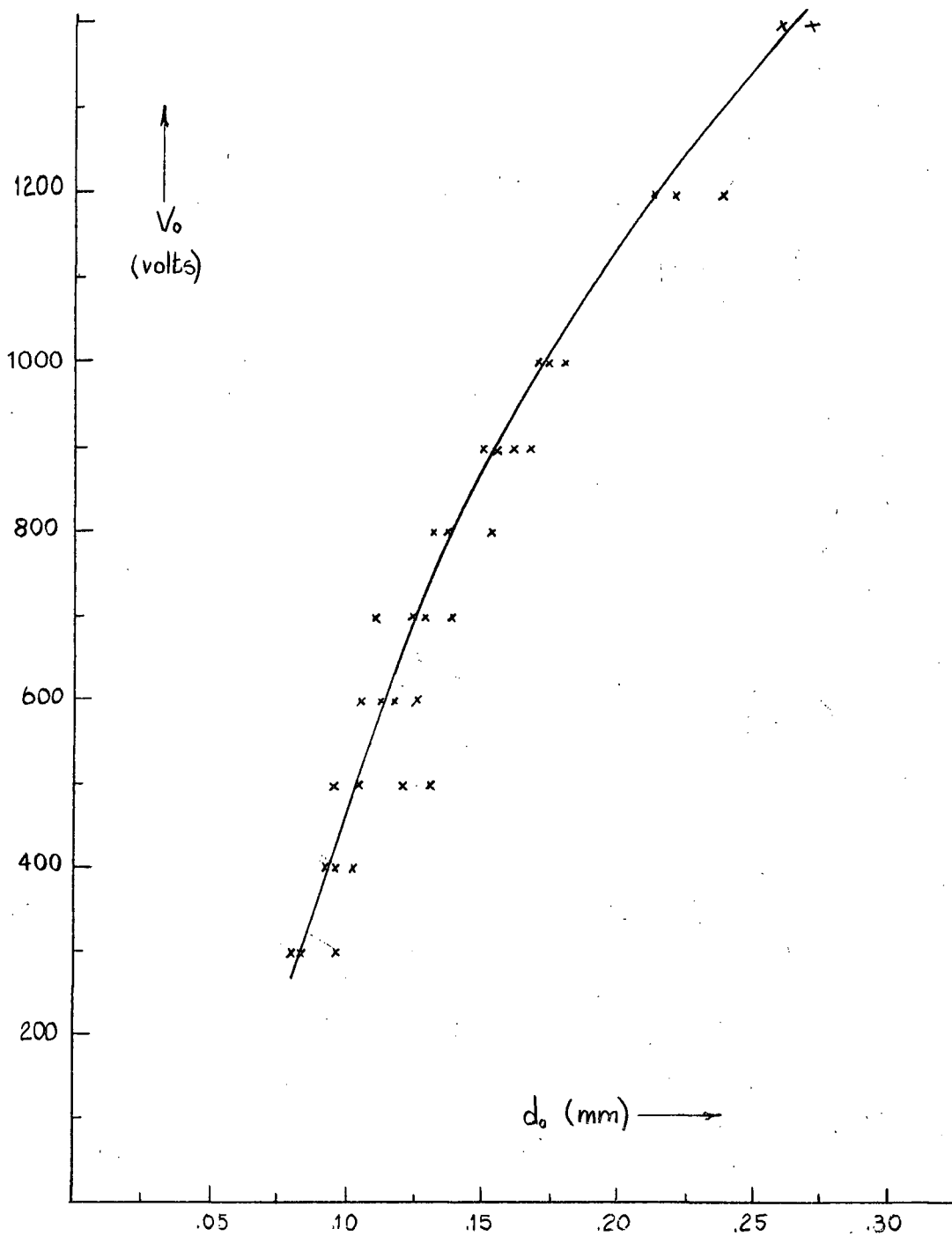
Figure 9   Paschen Curve

Spark breakdown in Argon gas (with Hg
vapour) at atmospheric pressure with
"hemisphere-plane" Hg electrodes.

to be quite impractical with the apparatus used in this experiment. For as the charging voltage increased, the gap separation decreased due to electrostatic attration of the two liquid surfaces. This difficulty made it impossible to obtain more than one particular voltage for a certain gap separation.

For these special conditions it was found more convenient to fix the voltage, and then observe the corresponding breakdown distance. This approach was used to determine the Paschen curve plotted in Figure 9. The gap separation could be controlled with a fair degree of sensitivity by means of the level control device inserted into vessel P.

2.4 TWO TYPES OF ARC TERMINATION

In the course of the experiment different values of R and V_o were used. Examination of the current and voltage traces indicated that there were two possible mechanisms by which the arc could be terminated. Although termination by either method occurred at times much later that the times at which the measurements were taken, it was felt that an investigation of the two mechanisms would lead to a better over-all understanding of the phenomena occurring in this particular arc.

The two cases of arc termination can be viewed in a complementary manner. The first is essentially an open-circuiting of the arc, while the second is essentially a short-circuiting of the arc.

The open-circuit occurs as a result of the RC decay of energy from the capacitor bank. When the voltage applied to the arc from the condensor falls below V_{min} (see Figure 2),

the arc extinguishes and the column plasma decays. Thus we refer to this phenomenon as the "Extinction" case.

The short circuit is the net result when the two liquid electrodes come into contact with each other. The mechanism responsible for this effect will be referred to as the "Shutting" mechanism.

(i) Extinction

Oscillograms of the current and voltage waveform indicating the extinction case of the arc are shown in Figure 10. At the extinction time t_e, the current ceases abruptly, and all of the voltage present on the condensor suddenly appears across the electrodes. This means that the electrode voltage jumps from V_{min} to the value $V_{min} + I_e R$, where $I_e R$ is the voltage across R just before the extinction. The voltage waveform clearly shows this jump effect (for the case of $R = 1\Omega$).

Referring to Fifure 7 we can determine the capacitor voltage as a function of time. Application of Kirchhoff's Law leads to

$$\frac{Q}{C} - I\left(R + R_a\right) = 0 ,$$

where,   Q = charge left on capacitor as a function of time

$I = -\dfrac{dQ}{dt}$ = current through circuit

R_a = ohmic resistance of the arc.

The voltage drop across L_i and R_c has been neglected. This differential equation has the standard solution for the capacitor voltage

$$V_c = V_o \exp - \int_0^t \frac{dt'}{C(R + R_a)}$$

V(t)

↓

↑

I(t)

t ⟶
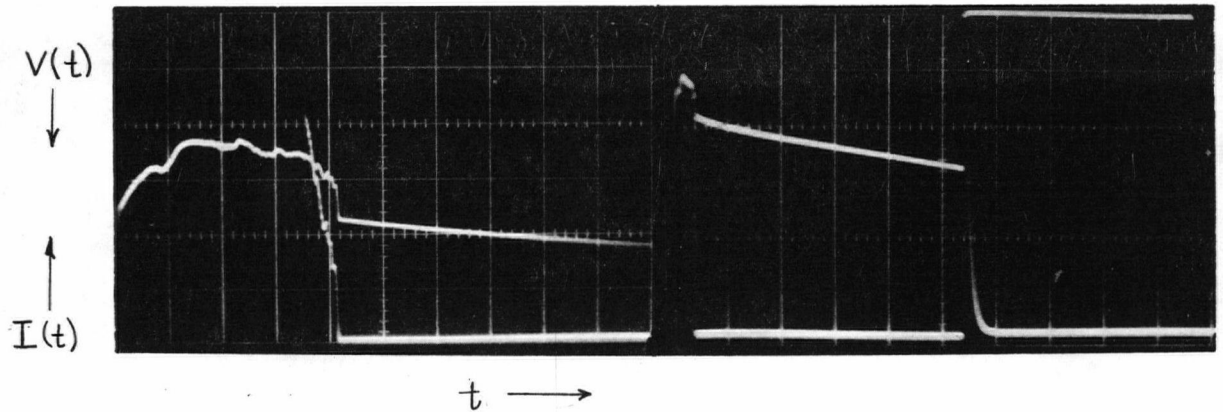
time (.2 msec/cm)   time (2 msec/cm)
voltage (5 volt/cm)   voltage (10 volt/cm)
current (2 amp/cm)   current (10 amp/cm)

voltage zero at top of oscillograms
current zero at bottom of oscillograms
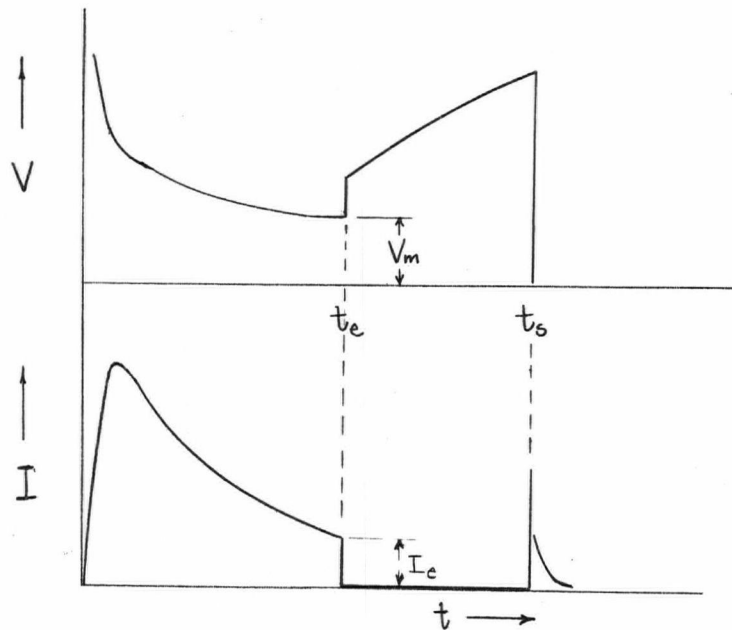
Figure 10   Extinction Mechanism

Both oscillograms taken with R = 5 Ω
and V_o = 600 volts.
Lower diagrams are schematic waveforms
which are not drawn to scale.
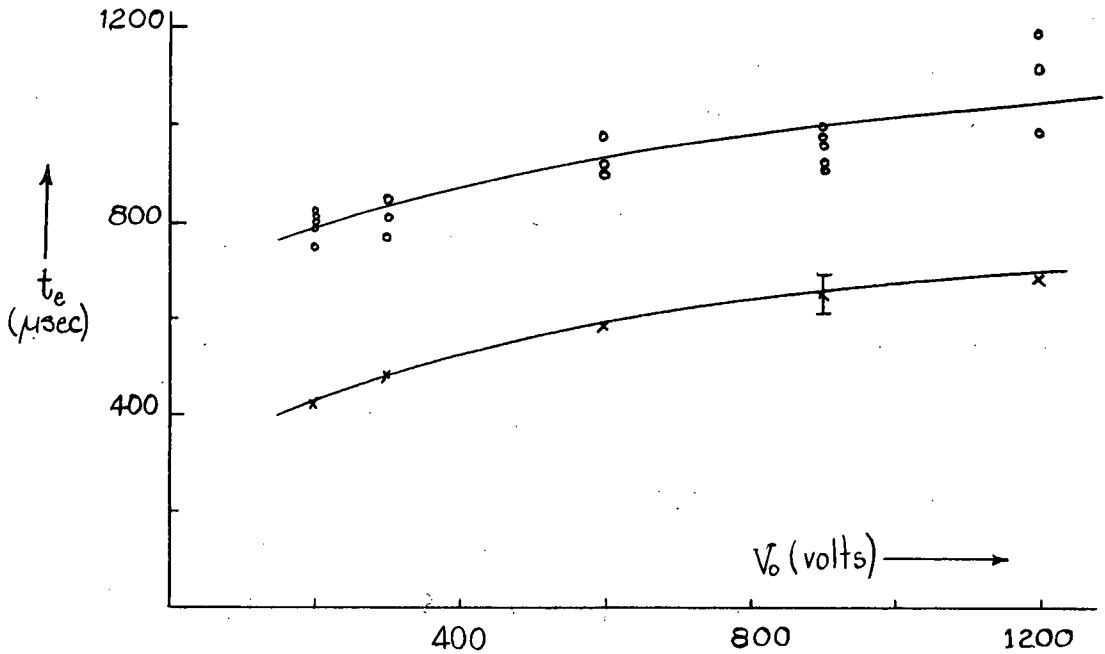
Figure 11 Extinction Time Dependence upon V_o

Experimental Values ($\circ$), with R = 5Ω;
Values determined by means of Equation 5 ($\times$),
with $V_c(t_e)$ = 12 volts as the average value.

where V_o is the initial voltage on the capacitor bank. Taking

natural logs of this expression at time t_e we obtain

$$\int_0^{t_e} \frac{dt'}{C(R + R_a)} = \ln \frac{V_o}{V_c(t_e)} . \qquad \dots(4)$$

The series resistor R remains constant throughout the interval

of integration as does the capacitor C, however, the arc resis-

tance varies approximately from zero to infinity (an open cir-

cuit at time t_e) in this period. If the approximation $R \ll R_a$

is used over the interval of integration we can determine a

simple expression for the extinction time,

$$t_e = RC \ln \frac{V_o}{V_c(t_e)} = RC \left\{ \ln V_o - \ln V_c(t_e) \right\}. \qquad \dots(5)$$

This expression was used, together with an average value of $V_c(t_e)$ to calculate t_e as a function of V_o, and the results are shown in the lower curve of Figure 11. The variation in $V_c(t_e)$ is shown schematically, but as $V_c(t_e)$ V_o in all cases the error introduced by using an average value will not be too large. The upper curve of Figure 11 shows the experimental points observed.

It can be seen that our simple model predicts values too low by approximately 35%. This error is mainly due to the fact that R_a was changing throughout the discharge. To perform a more careful check on equation 4, it was necessary to determine R_a as a function of time. This calculation was completed for two points (one is shown in Appendix B), and equation 4 was experimentally verified to within 10%.

(ii) Shutting

Observing an arc voltage waveform for the case of a small R and high V_o, it was noted that there was a sudden drop to zero at a time t_s (referred to as the shutting time). If this drop was the result of the two electrodes touching each other, a corresponding increase in the current should be observable. Using a high sensitivity current probe, it was found possible to observe this simultaneous current increase. Figure 12 shows a typical oscillogram of the shutting mechanism.

On first view, it is not understandable why the electrodes should move together during the discharge, as they remain separated indefinately when the apparatus is not in use. An examination of all forces acting on the bubble surface must be undertaken in order to understand this motion. These include;
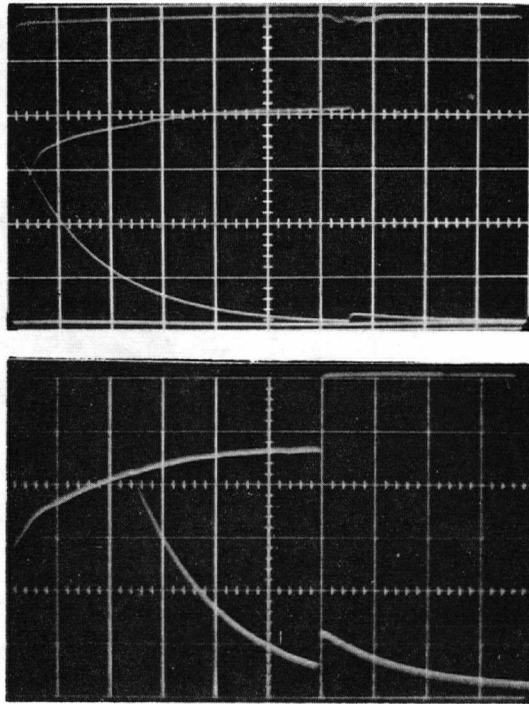
Figure 12   Arc Termination by Shutting

>Dual-beam oscillograms with upper trace
>displaying voltage (5 volt/cm with zero
>at top of both oscillograms), and lower
>trace displaying current (50 amp/cm and
>10 amp/cm in upper and lower oscillograms
>respectively). Both oscillograms were
>taken with horizontal sweep of 20 μsec/cm
>for the case of V_o = 200 volt, and R = 1Ω.

surface tension, gravity, and electromagnetic forces. An order

of magnitude calculation quickly shows that the gravitational

force could not be the main force drawing the upper electrode

down to the lower one. And the surface tension force can be

neglected because this force would tend to impede the motion

of the upper electrode. It is probable that the main force

is due to the electromagnetic $\underline{j} \times \underline{B}$ force acting on all current carrying parts of the circuit.

This pinch-like force would have most effect upon the narrow cylindrical upper electrode. As the Hg is almost incompres-sible, and as the bottom portion of the upper electrode is disturbed due to the passage of current, it would appear conceivable that a column of Hg is forced out towards the cathode as a result of this pinching force. This motion would then establish a liquid Hg bridge between anode and cathode at time t_s, and hence, would effectively short-circuit the arc.
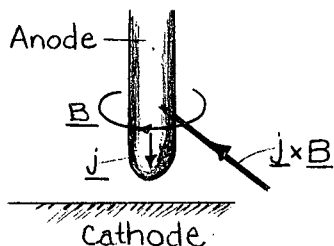
Figure 13   Electromagnetic Force

As both $\underline{j}$ and $\underline{B}$ are directly proportional to the current I, the electromagnetic force is proportional to I^2. The current is given approximately by

$$I(t) \cong \frac{V_o}{R} e^{-t/RC} .$$

This expression follows from the previous section on extinction for the case of $R \gg R_a$. Thus, it can be seen that the electro-magnetic force is proportional to $(V_o/R)^2$, and has an impulsive character due to the exponential factor $e^{-2t/RC}$.

Using Newton's Law an expression can be determined which qualitatively indicates the dependence t_s may have upon the different circuit parameters. Consider

$$F_{em} = m\ddot{x} = \lambda I^2,$$

where F_{em} is the electromagnetic force, and λ is the factor of
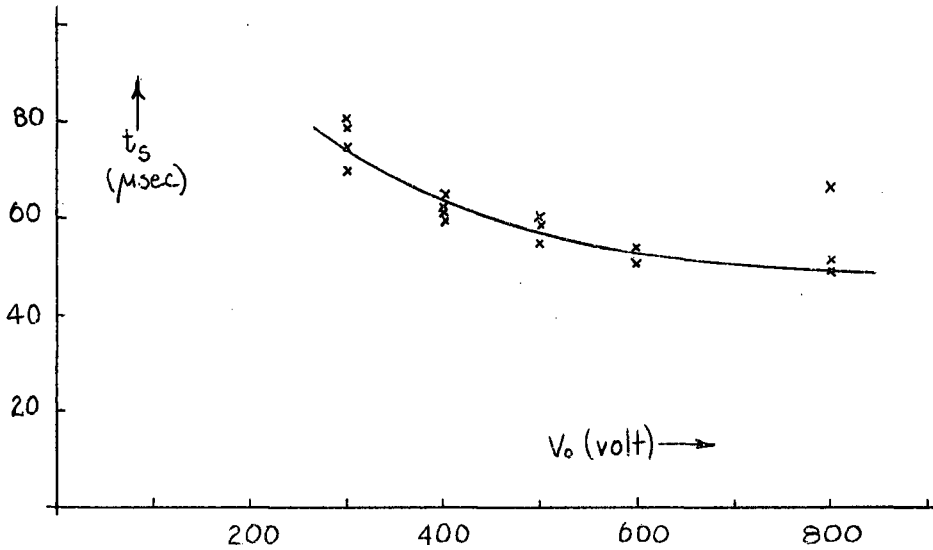
Figure 14 Shutting Time Dependence upon V_o

Experimental points with R = 1/2 Ω
and C = 30 μf.

proportionality. Integrating this expression twice we obtain

$$\dot{x}(t) = \frac{aV_o^2 C}{2R}\left\{1 - e^{-2t/RC}\right\} \qquad \ldots(6)$$

and,

$$x(t) = \frac{aV_o^2 C}{2R}\left\{t - \frac{RC}{2}(1 - e^{-2t/RC})\right\} \qquad \ldots(7)$$

with a = λ/m. Generally, $t_s \geqq 2RC$, so that $e^{-2t_s/RC} \ll 1$, and

hence it follows,

$$x(t_s) = \frac{aV_o^2 C}{2R}\left\{t_s - \frac{RC}{2}\right\}.$$

Now $x(t_s)$ is the distance travelled by the upper electrode in

the time t_s, and hence is just the initial gap separation d_o,

given by the Paschen curve. Substituting, and rearranging for

t_s gives,

$$t_s = \frac{RC}{2} + \frac{2Rd_0}{aV_0^2C} \quad .$$

As neither λ nor m can be determined, and as both have been assumed to be constant, the above expression for t_s must be viewed strictly in a qualitative sense. In this respect it is more reasonable to use

$$t_s \propto Rd_0/V_0^2 \qquad \qquad \ldots(8)$$

as the final expression for the shutting time.

The dependence upon R and V_0 was verified experimentally and one case is shown in Figure 14. The large amount of scatter obtained is to be expected when the scatter in the Paschen curve is taken into consideration.

An interesting point arose when examining the I-V trace (obtained with an x-y oscilloscope) of a discharge terminated by the shutting mechanism. After shutting had occurred there was a relatively linear decrease of voltage with current in time. The resistance indicated by the slope of this curve was found to be $4 \times 10^{-2} \Omega$ - approximately $3 \times 10^{-2} \Omega$ larger than the value of R_c measured in section 2-2. This added resistance could be interpreted as the resistance of the Hg column proposed by the shutting mechanism. If so, it would then correspond to a Hg cylinder of height d_0 and cross-sectional area of the order 5×10^{-5} cm^2.

(iii) Extinction versus Shutting

Having proposed models for the two arc termination possibilities, we should now examine the conditions under which

extinction or shutting is to be expected. It is clear that if

shutting precedes extinction (as is the case whenever $t_s < t_e$),

then extinction cannot possibly occur. However, for the case

of extinction preceding shutting $(t_e < t_s)$, the usual shutting

should still be observed as the $\underline{j} x \underline{B}$ forces are still present.

Upon examination with a long time scale this was found to be

true.

Consider the schematic diagram illustrating the dependence

of t_s and t_e upon V_o. It can be

seen that for voltages less than

V_{01}, $t_e < t_s$, and so extinction

should prevail. Similarly, for

voltages higher than V_{01}, then

shutting should prevail. This

tendency was experimentally found -

however V_{01} was very poorly de-

fined. This was probably a result of the low slope of the t_s

and t_e curves, and also due to the high scatter of the Paschen

curve.

Figure 15 Extinction or
           Shutting

While the value of V_o was shown to be a factor in deter-

mining which of the two mechanisms would terminate the arc, it

was soon noticed that the choice of R played a much more impor-

tant role in this determination. It was found that low R

values favoured shutting, while higher R values generally pre-

ferred extinction. According to the expressions derived for

t_s and t_e, this feature was not expected as both times are

directly proportional to R. The failure to explain this exper-

imental result is an unexplained short-coming of the proposed
models.

(iv) Independent Evidence for the Motion

To perform an experiment which would give some support to
the proposal of the shutting mechanism a modification was made
in the design of the apparatus. The upper Hg electrode was
replaced by a solid brass electrode. A resistor of $.6\Omega$
was used in series with the capacitor bank which was initially
charged to V_o = 1000 volts. These conditions ensured that
arc termination would occur by shutting mechanism whenever
the upper electrode was liquid Hg. However, as a solid elec-
trode would not distort under the action of the $\underline{j}x\underline{B}$ forces, it
was expected that only extinction would be observed.

The results of this experiment were very encouraging.
The shutting, which would have occurred at a time less than
100 μsec, was not observed. Instead, extinction terminated
the arc at a time around 200 μsec - a reasonable value of t_e
for these parameters.

As Jones and Galloway (1938) mention that solid electrodes
in Hg discharges tend to become covered with a thin Hg film,
the anode was carefully cleaned for each important discharge.
This precaution was found to be necessary, for after several
shots had taken place, the terminating mechanism suddenly
changed to shutting.

2.5 RELATIVE VELOCITY OF THE ELECTRODES

As previously mentioned in the Paschen curve section, the
electrode separation is an important parameter of an arc which

should be determined. The initial distance was measured by
determining the Paschen curve, but as the upper electrode
moved towards the lower one in the course of a discharge, it
is clear that this distance was constantly changing. For this
reason it was necessary to make some estimate of the relative
velocity between the surfaces before reliable data could be
extracted from the waveforms obtained.

The average velocity over the total discharge time can be
obtained by dividing the breakdown distance by the shutting
time. Using the standard case of $R = 1\Omega$, the shutting time
was found to vary from 150-100 μsec as the breakdown voltage
varied from 300-800 volts. The corresponding values of break-
down distance could be found on the Paschen curve, and the
resulting variation in the velocity was approximately 60-140
cm/sec. In agreement with the shutting mechanism proposal the
average velocity increases with increasing breakdown voltage
(see equation 6).

The final velocity v_f could be estimated by means of equa-
tions 6 and 7. At time t_s, $\dot{x}(t_s) = v_f$, $x(t_s) = d_o$, and by di-
viding and rearranging it then follows that

$$v_f = \frac{d_o}{t_s - RC/2} . \qquad \qquad ...(9)$$

This result appears reasonable, as v_f is larger than the average
velocity d_o/t_s, but it should be stressed that this calculation
involves drastic approximations. With the identical conditions
used in the calculation of the average velocity, the variation
in v_f was found to be approximately 65-160 cm/sec.

An independent check on the motion of the electrodes was obtained when a large inductance L (32 μH) was placed in series with the arc. The current then increased slowly, and the voltage for the same current could be measured at two times (t_1, $t_2 \doteq 2$ μsec) after the arc plasma had been established. The observed decrease in voltage $\Delta V = V(t_1) - V(t_2)$ could be attributed to a decrease in the arc column length. This was caused by the motion of the electrodes as shown in the following brief discussion.

The total voltage drop across the electrodes is given by

$$V = V_c + V_{co} + V_a$$

in accordance with figure 3. Taking the first time derivative of this equation gives

$$\frac{dV}{dt} = \frac{dV_c}{dt} + \frac{dV_{co}}{dt} + \frac{dV_a}{dt}$$

which approximates to

$$\frac{dV}{dt} = \frac{dV_{co}}{dt}$$

because the fall voltages are insensitive to changes in both the current (Gerthsen and Schulz, 1955), and the electrode separation (we inherently assume that the arc is sufficiently long to establish a column). The column field strength

$$E_{co} = \frac{dV_{co}}{dx}$$

is approximately constant over the column (see figure 3), but is highly dependent upon the current. Assuming that E_{co} is
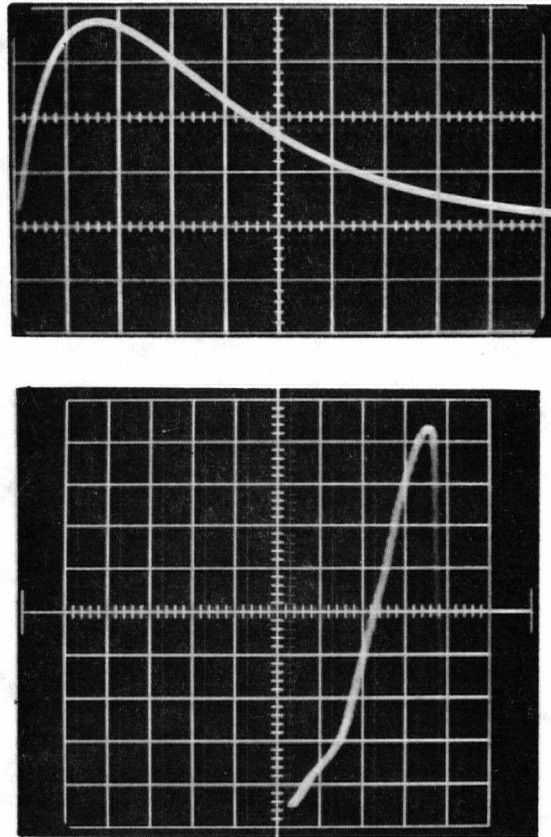
Figure 16   Determination of Electrode Velocity

Oscillograms were taken simultaneously on
two different oscilloscopes for the case
of R = 2Ω, C = 30 μf, V_o = 600 volt.

Upper trace: current (50 amp/cm with zero 2 cm
above bottom line) versus time (20 μsec/cm).

Lower trace: current (20 amp/cm with zero on bot-
tom line) versus voltage (2.5 volt/cm with
zero 1 cm from left hand border).

unaffected by a slight motion of the electrodes, then for a fixed

current we have the following

$$\frac{dV_{co}}{dt} = \frac{dV_{co}}{dx}\frac{dx}{dt} = E_{co}v$$

or,

$$v = \frac{1}{E_{co}}\frac{dV}{dt} \cong \frac{1}{E_{co}}\frac{\Delta V}{\Delta t} \; . \qquad\qquad ...(10)$$

Using the parameters, L = 32 μh, R = 2Ω, C = 30 μf, and

V_o = 600 volt, the oscillograms shown in figure 16 were obtained.

From these traces $\frac{\Delta V}{\Delta t}$ can be obtained for several values of a

fixed current. Then, taking the corresponding column field

strength for these currents from figure 18, the average velocity

over the interval $\Delta t = t_2 - t_1$ could be determined. A typical

case was at I = 175 amp where Δt = 33 μsec, ΔV = 1.1 volt,

thus giving v = 62 cm/sec. This figure is reasonable consider-

ing the experimental conditions.

Although no exact determination of v could be made, the

reasonable agreement between the three approaches indicated that

the relative velocity is of the order of 100 cm/sec. With this

figure in mind it would appear reasonable to assume that if

measurements for a particular V-I characteristic are taken in

the first 2-15 μsec of a discharge, then the electrode separation

should vary less than 10% from the measured breakdown distance.

CHAPTER 3 - GENERAL MEASUREMENTS OBTAINED

3.1 ELECTRODE FALL REGIONS

An order of magnitude value for d_f and E_f (the average value of field strength in the fall regions), could be obtained by observing the voltage waveform near the time of shutting t_s. As the relative velocity of the electrodes at t_s may be found from Equation 9, the total thickness of the fall regions may be determined by measurement of the time τ taken for the voltage to drop to zero. The average field strength in the fall region may then also calculated.

By using the 545 - oscilloscope on the delayed triggering mode it was possible to measure this time τ. For the standard case of $R = 1\Omega$ and $V_o = 400$ volts, a value of $\tau = 40$ nsec was measured as shown in Figure 17. As the rise time of the oscilloscope and pre-amp. is approximately 10 nsec, this value of τ should be 3% higher than the actual value.

Using Equation 9 with $t_s = 140 \mu sec$, $d_o = 9 \times 10^{-3}$ cm, (values which correspond to the case of $V_o = 400$ volts), the shutting time was calculated to be 72 cm/sec. The total fall distance is given by

$$d_f = v_j \tau$$

and was found to be 2.9×10^{-6} cm. Then E_f is determined in a similar manner by the equation

$$E_f = \frac{V_f}{d_f} = \frac{V_f}{v_j \tau}$$

and was found to be 2.4×10^6 volt/cm, using $V_f = 7.5$ volt (this was the average value accurate to $\pm .5$ volt).
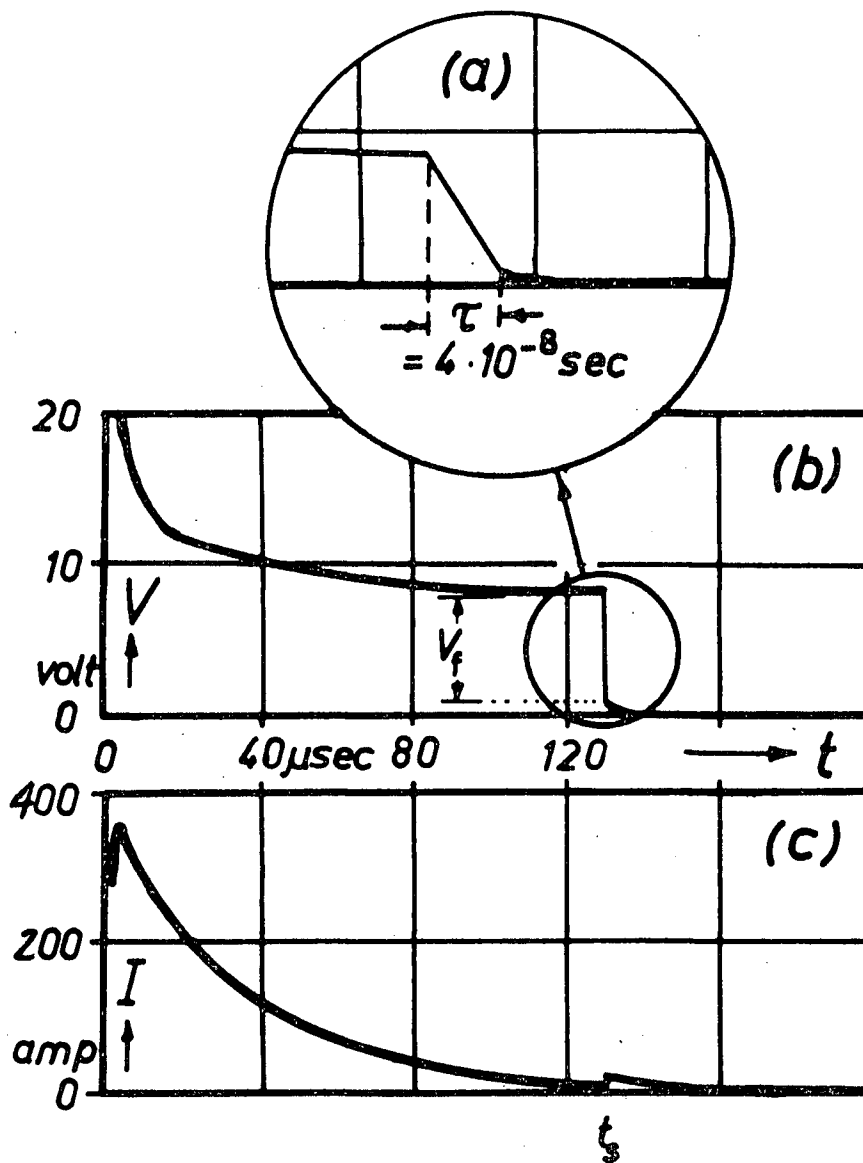
Figure 17   Voltage and Current Waveforms

Graphical enlargements of three
oscillograms taken with $R = 1\,\Omega$,
$C = 30\,\mu f$, and $V_0 = 400$ volts.

As indicated in Chapter 1 it is the value of E_c rather than E_f which is of importance to the general theory of arc physics. According to Gerthsen and Schulz (1955), the cathode drop is about ten times that of the anode drop, and so

$$E_f = \frac{V_a + V_c}{d_a + d_c} \cong \frac{10}{9} \frac{V_c}{d_a + d_c}$$

Then by substituting the expression for E_c (note this is only the average value again) and rearranging we obtain

$$E_c \cong \frac{d_a + d_c}{d_c} \frac{9}{10} E_f = \frac{9}{10} \left\{ 1 + \frac{d_a}{d_c} \right\} E_f$$

Thus, we see that although 2.2×10^6 volt/cm is the minimum value for E_c, values of 10^7 volt/cm and higher are possible depending upon the ratio d_a/d_c.

3.2 COLUMN FIELD STRENGTH

The simultaneous measurement of current and voltage together with the Paschen curve could be used to determine the column field strength E_{co} over the total column length to be calculated.

E_{co} may be determined only during the initial stages of the discharge (2 μsec $\leqq$ t $\leqq$ 15 μsec), when the change of electrode separation is small compared with d_o. Then, since $d_f \ll d_o$

$$E_{co} \cong \frac{V - V_f}{d_o}$$

where V is the total voltage across the electrodes. A correction had to be made to V for the voltage drop across R_c as measured in Section 2.2.

The average value of V_f = 7.5 volts was used in all calculations. The use of a constant value should be a good approxi-

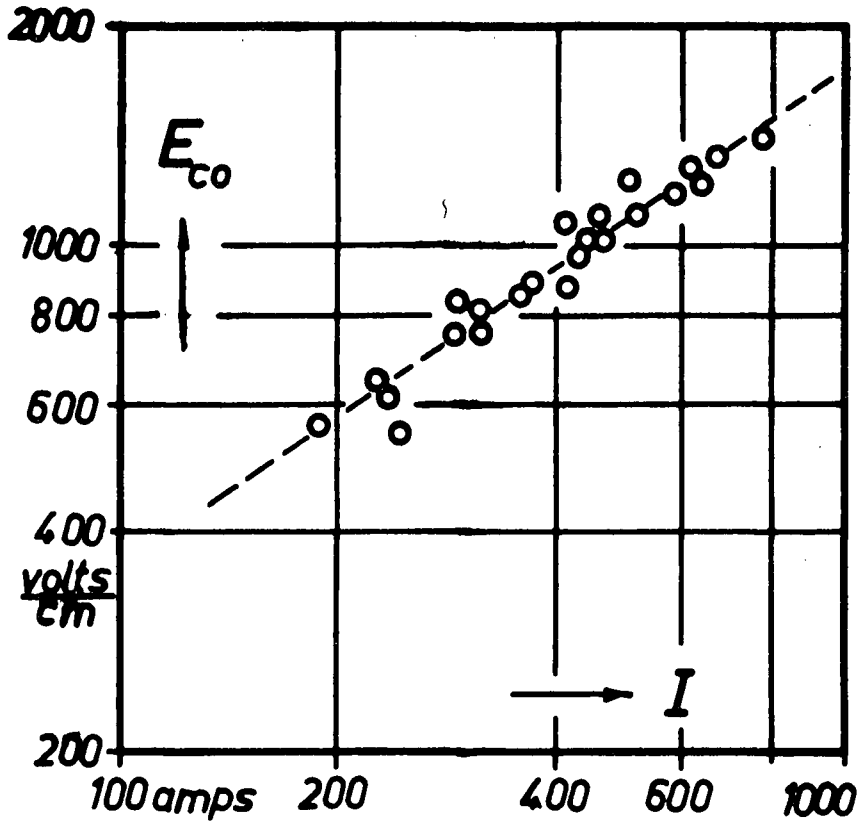Figure 18   Column Field Strength Dependence
            upon Current

mation according to Bauer and Schulz (1955), who found that for

high currents (say greater than 100 amp) the fall voltages as-

sumed constant voltages.

Figure 18 shows the result of plotting E_{co} as a function

of current (on log-log paper). The slope of the curve is .66,

which indicates a relation

$$E_{co} \propto I^{.66} \quad .$$

This result is very different from that obtained by Maecker (see Chapter 1). The apparent discrepancy is probably a consequence of two features of Maecker's theory which should be mentioned. First, his derivation completely neglects radiation losses, which may be the major energy dissipation mechanism in this particular arc. Second, the effect of the dynamic aspects will not be accounted for in the d.c. model developed by Maecker.

3.3 VOLTAGE-CURRENT CHARACTERISTIC

The initial objective of this thesis was to obtain the overall V-I characteristic for an arc and to compare these measurements with the results derived by Smy (see Chapter 4). Two methods were used to obtain the characteristic; the first, a direct plotting of measurements obtained from the oscillograms; the second, a combining of several different oscillograms to give a single reduced characteristic. Both approaches lead to similar results — the reduced characteristic extending over a larger current range than did the direct plot.

(i) Reduced Characteristic

As discussed in Chapter 2, the arc was initiated by a sparking mechanism according to the Paschen curve. If only the first 2 - 15 μsec of the trace were to be used, then the current range obtained for a particular breakdown distance would be relatively small (see Figure 17). To increase the current range, a different initial maximum current could be used, and this could be obtained only by changing the breakdown voltage. However, a change in V_0 is accompanied by a change in d_0, and this would then mean that we were examining a different characteristic determined by
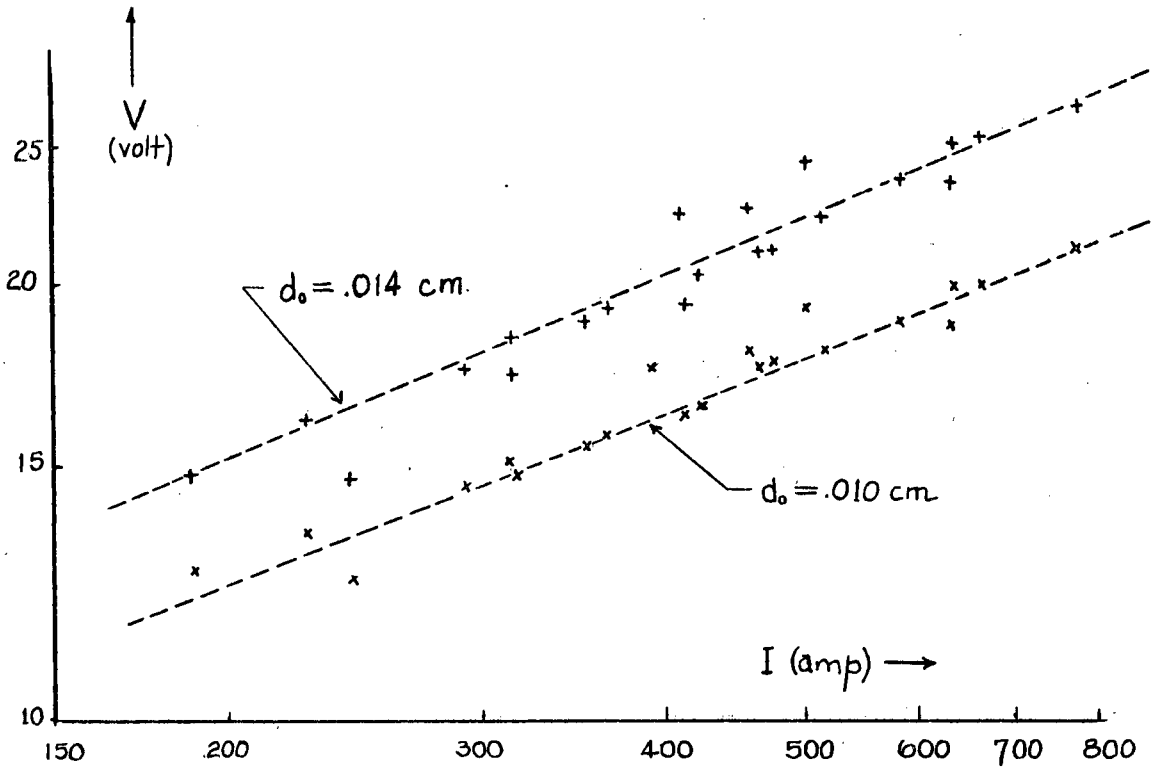
Figure 19   Reduced V-I Characteristics

this new separation (see Figure 2).

Choosing some intermediate value of electrode separation, say d_1, an approximate reducing technique was used to convert the characteristic obtained for a different separation, say d_2, into a modified characteristic which would correspond to the chosen value of d_1. Consider some point (V_2, I_2) on the d_2 characteristic which is to be reduced to the d_1 characteristic. The reduced point is designated as (V'_2, I'_2), where,

$$I'_2 = I_2,$$
$$V'_2 = V_2 - \Delta V_2,$$

$$\Delta V_2 = -\frac{d_{21}}{d_2}\left\{V_2 - 7.5\right\},$$

$$d_{21} = d_2 - d_1 \; .$$

It follows that

$$V_2' = \left\{V_2 - 7.5\right\}d_1/d_2 + 7.5 \; .$$

This technique is identical to that used in section 3.2, the essential assumption being that there is a linear gradient in the potential variation across the column region. The same average value of $V_f = 7.5$ volts was used in all calculations again.

Reduced characteristics were calculated for the two cases shown in Figure 19, and the average slope of the curve indicated an impedance relation of the form

$$V \propto I^{.44} \; .$$

(ii) Direct Characteristic

The results obtained by directly measurements from the V-I traces (see Figure 20) are shown in Figure 21. Initially, only measurements in the first 15 μsec were taken. However, upon further examination it was found that the characteristic remained very linear over a longer period of time. This indicates that the arc is stable over a period of 30 μsec rather than the 15 μsec obtained in section 2.5. The average slope for the three cases plotted gave the experimental result

$$V \propto I^{.43} \; .$$

(iii) Summary of Both Approaches

The results of both approaches can be described by the
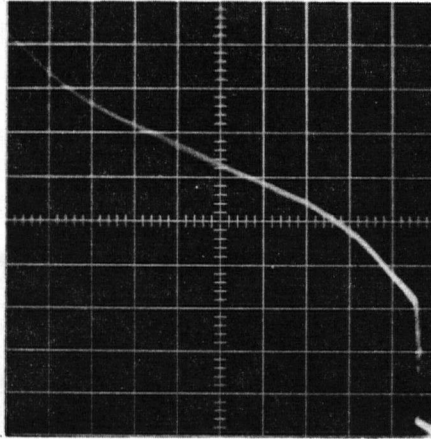
Figure 20 Voltage-Current Oscillogram

Voltage (2.5 volt/cm) versus current (40 amp/cm) with origin in lower right hand corner, for the parameters $R = 1\Omega$, $C = 30\,\mu f$, $V_0 = 500$ volt.
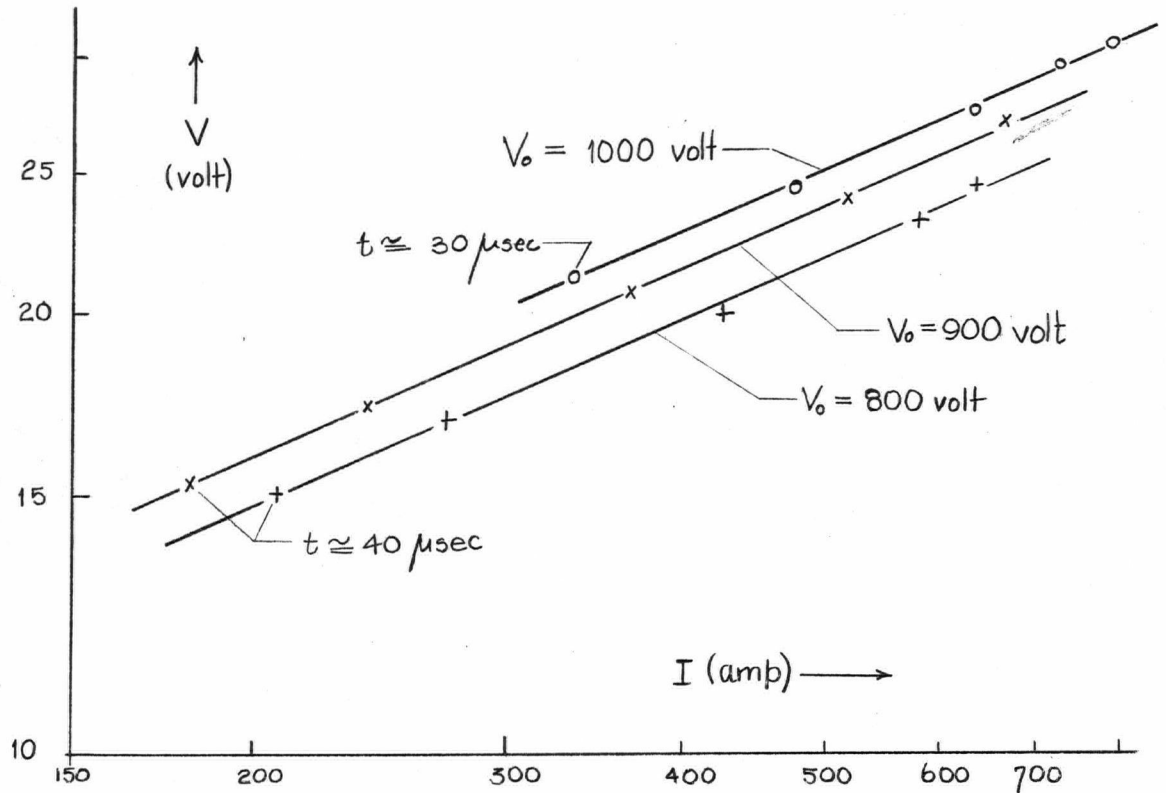
Figure 21 Direct V-I Characteristics

equation

$$V = kI^{.43},$$

where the constant k is dependent upon the electrode separation.

This experimental result is very similar to the relation $V \propto I^{.4}$ developed by Smy. In order to see whether or not this result should be a general feature of arcs (and not just an incidental similarity) the following chapter will present an examination of the derivation and assumptions involved in Smy's theory.

CHAPTER 4 - SPOT CONDUCTION MODEL OF THE ARC

4.1 DEVELOPMENT OF THE MODEL

The current-voltage relationship derived by Smy (1963), was originally developed to determine the impedance between two electrodes immersed in a shock heated plasma. The essential features of this theory are very similar to generally accepted ideas in arc physics. The total arc voltage was considered to be made up of two components; the voltage across the cathode spot V_s, (which is equal to the cathode fall voltage Vc), and the ohmic voltage drop across the intervening plasma V_p. It was found that both V_s and V_p were dependent upon the spot area, and that there existed a possible optimum area for which the total arc voltage was a minimum. This optimization resulted in the final expression

$$V_{min} \propto I^{.4}$$

which was shown to give order of magnitude agreement with the experiments conducted by Smy and Driver (Smy, 1963; Driver, 1964).

(i) Spot Voltage

The main experimental observation by Smy which lead to his theory was the occurrence of a particular voltage regime in which the current-voltage characteristic was independent of the electrode area. This was shown to be so by placing electrodes of various sizes across the shock tube for both increasing and decreasing currents. The proposal of a small conducting spot analogous to that which arises in arcs was found to be very successful in explaining the unusual features of the observed characteristic. As the objective of this chapter is to

examine how well Smy's theory applies to an arc, the details and plausibility arguments for the conducting spot in the shock tube have been omitted (for details see Smy, 1963). This was done because the phenomena of spot conduction in an arc has been well accepted (see Froome, 1950). Using Mackeown's field emission equation (see Chapter 1) and assuming typical values for E_c and γ, the spot voltage is related to the spot area A_s by

$$V_s = k_1 j^{-2} = \frac{k_1}{I^2} A_s^2 \; , \qquad \ldots(11)$$

with k_1 constant.

(ii) Plasma voltage

The expression for the resistance of the intervening plasma was derived in accordance with standard electromagnetic theory (Smythe, 1950). Assume that an infinite, isotropic medium of constant resistivity ρ separates two conductors A, and B. If the separation distance ℓ, is large compared to a typical length of the conductors, then it can be shown that the resistance of the intervening plasma is given by

$$R_p = \rho\left\{ \frac{\epsilon_o}{C_A} + \frac{\epsilon_o}{C_B} - \frac{1}{2\pi\ell} \right\} \qquad \ldots(12)$$

where C_A, C_B are the capacities of the two isolated conductors A, B respectively. Taking conductors A and B to refer to the negative and positive electrodes respectively, then C_A would be the effective capacity of the cathode spot. If an identical spot was formed on B, then $C_A = C_B$. However, the occurrence of such an anode spot was thought to be unlikely (in analogy with an arc again), and so C_B^{-1} was neglected in comparison

with C_A^{-1}. The capacity of a thin disc of radius r is given by

$$C_d = 8\varepsilon_o r$$

according to standard tables (Handbook of Chem. and Phys., 1964). Assuming a circular cathode spot forms on the negative electrode, then

$$C_A = \frac{C_d}{2} = 4\varepsilon_o \sqrt{\frac{A_s}{\pi}}$$

as only one face of the "cathode disc" is in contact with the plasma. Now the plasma resistance is given by

$$R_p = \rho \left\{ \frac{1}{4} \sqrt{\pi/A_s} - \frac{1}{2\pi l} \right\}$$

and the plasma voltage is then given by

$$V_p = IR_p.$$

(iii) Total Voltage

The total arc voltage can now be determined by taking the sum of V_s and V_p,

$$V = \frac{k_1}{I^2} A_s^2 + \frac{I\rho}{4} \sqrt{\pi} A_s^{-\frac{1}{2}} - \frac{I\rho}{2\pi l}$$

$$= \frac{k_1}{I^2} A_s^2 + k_2 I A_s^{-\frac{1}{2}} - k_3 I . \qquad \ldots(13)$$

For the case of Smy's shock tube the last term was neglible in comparison to the second term so that

$$V \cong V_{st} = \frac{k_1}{I^2} A_s^2 + k_2 I A_s^{-\frac{1}{2}} \qquad \ldots(14)$$

The power loss in the arc is given by the product IV. It is assumed that given sufficient time the spot area will adopt

that value which will minimize this loss by minimizing V for a
particular I. This optimum area can be determined by partial
differentiation of the voltage with respect to the area, giv-
ing the final result,

$$A_o = \left[\frac{k_2}{4k_1}\right]^{.4} I^{1.2} . \qquad \ldots(15)$$

Then the corresponding voltage for this particular area is
given by

$$V_{min} = \frac{5}{4^{.8}} k_1^{.2} k_2^{.8} I^{.4} - k_3 I . \qquad \ldots(16)$$

Examining Smy's shock tube approximation, it is found that
the optimum area remains unchanged, and so

$$V_{st,min} = \frac{5}{4^{.8}} k_1^{.2} k_2^{.8} I^{.4} . \qquad \ldots(17)$$

It is also worth noting that when optimum conditions have been
achieved, this approximation gives the interesting result that
the two voltages are in the ratio

$$\frac{V_s}{V_p} = \frac{\text{spot voltage}}{\text{plasma voltage}} = \frac{1}{4} . \qquad \ldots(18)$$

4.2 DISCUSSION

In Sec. 3.3 it was experimentally found that $V = kI^{.43}$,
and this result would appear to be in good agreement with Smy's
spot conduction model. However, upon detailed examination it
was shown that the agreement is only fortuitous, as there are
assumptions made in this model which cannot be satisfied by
our experimental arc.

It is easily shown that the shock tube approximation,
$\ell \gg A_o^{1/2}$ does not hold for our particular conditions. Consider

a typical case for a particular current maximum; the electrode separation can be determined by the Paschen curve, and the optimum area is given by Equation 15. For a current of 500 amp, it was found that $\ell \cong 10^{-2}$ cm, and $A_o^{1/2} \cong 10^{-1}$ cm. Another approach to determine a measure of the spot area is to assume an accepted value for the current density, say $j = 10^6$ amp/cm^2, then for $I = 500$ amp, $A^{1/2} \cong 10^{-2}$ cm. While the two approaches give values of $A^{1/2}$ which differ by an order of magnitude it is certainly evident that the approximation $\ell \gg A^{1/2}$ is invalid for this situation.

An important difference between the electric arc and the case of two electrodes immersed in a shock heated plasma gives rise to another reason which invalidates the use of the spot conduction model to describe the electric arc characteristic. The passage of current in the arc maintains the ionization in the gas, whereas in the shock tube the gas is already ionized and is constantly being replaced by the plasma flow. From this it can be seen that the assumption of an infinite isotropic plasma of constant resistivity may apply to the shock tube but will not apply to a regular arc. The current results in a radially dependent resistivity which has a minimum value along the axis of the current flow (see Maecker, 1959). It would be expected then that the expression for R_p would be modified — the net result being that the final expression for V_{min} would also be quite different.

CONCLUDING REMARKS

It was possible to measure several of the important variables of an arc with Hg electrodes, namely the Paschen breakdown curve, the overall voltage-current characteristic, and the column field strength dependence upon current. However, it must be stressed that these measurements are more of a qualitative than quantitative nature. The observed motion of the electrodes was the main factor contributing to this feature, and even though the motion was reasonably well established, its velocity could only be approximately measured.

The results obtained for the overall V-I characteristic were found to agree fairly well with the predictions of Smy's spot conduction theory. It was shown that this agreement was only fortuitous however, as many of the assumptions required for the derivation are not satisfied by conditions in this arc.

The observed motion of the Hg electrodes made possible an approximate determination of the combined thickness of the cathode and anode fall regions and the average field strength in these regions. Although the measured field strength is consistent with the predictions of field emission theory, the accuracy of the result does not allow acceptance of this theory beyond any doubt. The encouraging feature of this measurement, however, is that by an appropriate re-design in the apparatus, it might be possible to obtain an accurate measurement of the shutting velocity. If so, the results thereby obtained may be sufficient to completely accept (or reject) the field emission theory.

APPENDIX A   LCR SERIES CIRCUIT

The case of a capacitor C initially charged to some voltage V_O discharging current i through a resistor R and series inductance L describes the behavior of our basic measuring circuit very well. The resistance of the arc is much less than the current limiting resistor so that the 3 parameters R, C, L may be taken as constants for the analysis.
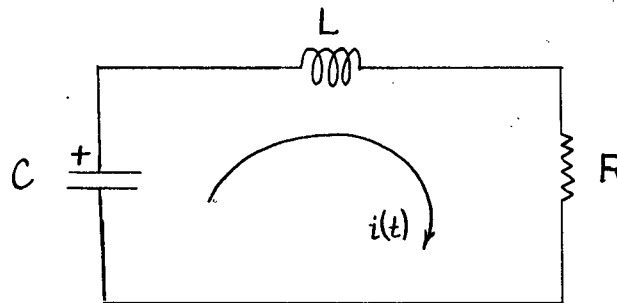

Figure 22   LCR Series Circuit

By application of Kirchhoff's Laws we obtain the differential equation for the current flow in the circuit,

$$\frac{d^2 i}{d t^2} + \frac{R}{L}\frac{di}{dt} + \frac{1}{LC} i = 0$$

which is subject to the initial condition i(0) = 0.

There are three current responses possible depending upon the relative magnitude of the circuit parameters. When the condition $R^2 > 4L/C$ is satisfied then the current response has the form

$$i(t) = \frac{V_0}{\sqrt{R^2 - 4L/C}} \cdot e^{-\frac{R}{2L}t} \left\{ e^{\frac{t}{2L}\sqrt{R^2 - 4L/C}} - e^{-\frac{t}{2L}\sqrt{R^2 - 4L/C}} \right\} .$$

(i) Current Waveform

All quantitative measurements were taken when the circuit components satisfied the inequality $R^2 \gg 4L/C$. Taking the equation for the current and using the linear approximation

$$\sqrt{1 - \frac{4L}{R^2 C}} \cong 1 - \frac{2L}{R^2 C}$$

we obtain,

$$i(t) \cong \frac{V_0}{R} e^{-t/RC} \left\{ 1 - e^{-Rt/L} \right\}$$

For times greater than $2L/R$ this equation reduces further to

$$i(t) \cong \frac{V_0}{R} e^{-t/RC}$$

which is the equation of a simple RC decay circuit. Typical current waveforms are shown in Figures 12 and 17, and a schematic of the waveform is given below.
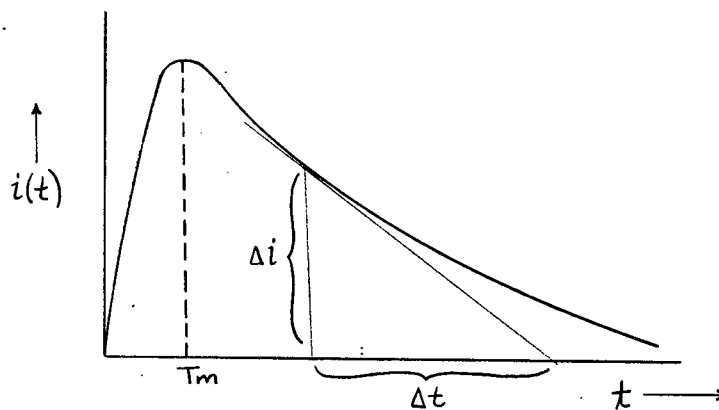

Figure 23   Current Waveform (schematic)

(ii) Resistance of the Arc

By performing a very simple measurement upon the current trace it was possible to determine the period of time in which the condition $R_{arc} \ll R$ was valid. An approximation of this time

was useful in the discussions of the shutting and extinction mechanisms of Chapter 2.

For any time $t > 2L/R$ draw the tangent to the curve and measure the slope which is given by

$$m = -\frac{\Delta i}{\Delta t} = -\frac{i(t)}{\Delta t} \ .$$

The slope of the simple RC decay waveform is given by

$$\frac{di}{dt} = -\frac{1}{RC}\frac{V_0}{R}e^{-t/RC} = -\frac{1}{RC}i(t) \ .$$

Hence, we see that $\Delta t = RC$ for an exact RC decay, and deviations from this value give a rough measure of the arc resistance . It was found for all cases that $R_{arc} \ll R$ for all $t \lessgtr 2RC$ by this technique.

(iii) Inherent Circuit Inductance

It was found that a measure of the inherent circuit inductance L_i, could be made by observing the time T_m of maximum current flow on the oscillogram. Taking the first derivative of the current (either one) and using the linear approximation shown in (ii) we obtain

$$T_m \cong \frac{L_i}{R} \ln \frac{R^2 C}{L_i} \ .$$

By measuring T_m, and substituting values for R and C, this equation can be solved either by graphical techniques or by an iteration technique for the value of L_i.

APPENDIX B GRAPHICAL EXAMINATION OF EXTINCTION

Referring to section 2.4 we had derived the equation

$$\int_0^{t_e} \frac{dt'}{C(R+R_a)} = \ln \frac{V_0}{V_c(t_e)} \qquad \ldots (4)$$

which simplifies to

$$t_e = RC \ln \frac{V_0}{V_c(t_e)} \qquad \ldots (5)$$

if the approximation $R \gg R_a$ holds in the time interval $0 \leqslant t \leqslant t_e$. As shown in Figure 11, the discrepancy between experimental results and Equation 5 was approximately 30-40 %. This disagreement suggested that a more careful examination of Equation 4 should be undertaken in which the approximation was not used.

By taking simultaneous current-time and voltage-time oscillograms of particular conditions it was possible to determine $R_a(t)$. Then by plotting the function $1/\{R + R_a\}$, and graphically integrating, it was possible to determine the value of the integral in Equation 4.

With the parameters $R = 5\,\Omega$, $V_0 = 300$ volts, the area under the curve was 1.04×10^{-4} sec/Ω as shown in Figure 24. Then the l.h.s. of Equation has the value 3.46 as $C = 30\,\mu f$. From the voltage waveform $V_c(t_e)$ was found to 12 volt, and so the r.h.s. of Equation 4 has the value $\ln(300/12) = 3.22$.

Although it is not possible to obtain a value for the expected extinction time, the agreement between both sides of the equation to within 7% is much more satisfactory than the results of Figure 11. It is also interesting to note that the dotted line of Figure 24 encloses the effective area which is used in
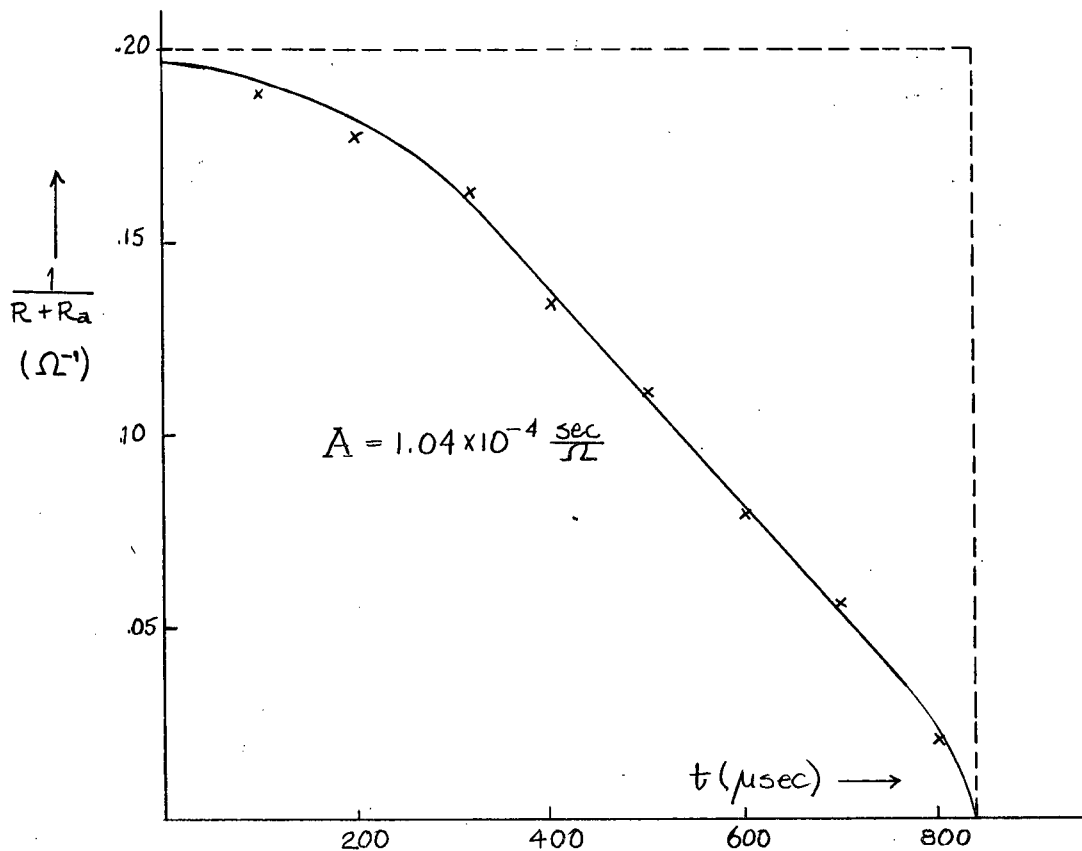
$$A = 1.04 \times 10^{-4} \frac{sec}{\Omega}$$

Figure 24   Graphical Integration of $\int \frac{dt'}{R + R_a}$

The parameters used were $R = 5\Omega$, and $V_o = 300$ volt.

in Equation 5, and it can be seen that the difference in the

two areas is of the same order of magnitude as the discrepancy

between the two curves of Figure 11.

BIBLIOGRAPHY

Ahlborn, B., Barnard, A.J., and Campbell, H.D. (1965) Canadian Journal of Physics.

Bauer, A. and Schulz, P (1954), Z.P. $\underline{139}$, 197.

Brown, S.C. (1961) "Basic Data of Plasma Physics", M.I.T. Press, Cambridge, Mass.

Driver, H.S.T. (1964) Ph.D. Thesis, University of British Columbia.

Ecker, G. (1961) Ergebn. d. exact. Naturw. XXXIII.

Engel, A. v. (1955) "Ionized Gases", Oxford, Clarendon Press.

Engel, A. v. and Robson, A.E. (1957) Proc. Phys. Soc. (London) $\underline{A243}$, 217.

Fowler, R.H. and Nordheim, L.W. (1928) Proc. Roy. Soc. (London) $\underline{A119}$, 173.

Froome, K.D. (1950) Proc. Phys. Soc. (London) $\underline{B63}$, 377.

Gerthsen, P. and Schulz, P (1955) Z.P. $\underline{140}$, 510.

Goldman, K. (1961) Proc. 5th Int. Conf. on Ionization Phenomena in Gases.

Handbook of Chemistry and Physics (1964-65).

Hinrichs, E. and Wienecke, R. (1959) Z.P. $\underline{156}$, 592.

Jones, L. and Galloway, (1938) Proc. Phys. Soc. $\underline{50}$, 207.

Mackeown, S.S. (1929) Phys. Rev. $\underline{34}$, 611.

Maecker, H. (1959) Z.P. $\underline{157}$, 1.

Schottky, W. (1925) Z.P. $\underline{31}$, 163.

Smy, P.R. (1963) Proc. Phys. Soc. $\underline{82}$, 446.

Smythe, W.R. (1950) "Static and Dynamic Electricity", McGraw Hill, N. Y.

Wasserab, T. (1951) Z.P. $\underline{130}$, 311.